Articles

Effect of Hydroxylation and N[187]-Linked Glycosylation on Molecular and Functional Properties of Recombinant Human Surfactant Protein A[†]

I. García-Verdugo,[‡,§] F. Sánchez-Barbero,[‡,§] F. U. Bosch,[ǁ] W. Steinhilber,[ǁ] and C. Casals*[,§]

Department of Biochemistry and Molecular Biology I, Complutense University of Madrid, 28040-Madrid, Spain, and Department of Biotechnology, ALTANA Pharma AG, Byk-Gulden-Strasse 2, 78467 Konstanz, Germany

Received May 3, 2003; Revised Manuscript Received June 27, 2003

ABSTRACT: The objective of this study was to determine the effects of proline hydroxylation in the collagen-like domain and Asn[187]-linked glycosylation in the globular domain on the molecular and functional properties of human surfactant protein A1 (SP-A1). To address this issue, SP-A1 was in vitro expressed in insect and mammalian cells. Insect cells lack prolyl 4-hydroxylase activity. A glycosylation-deficient mutant SP-A1 was expressed in insect cells. In this report we present evidence that hydroxylation increased the T_m of the collagen-like domain by 9 °C. Proline hydroxylation affected both the arrangement of disulfide bonding and the extent of oligomerization but did not affect conformational changes in the globular domain identified by intrinsic fluorescence. Both self-association and lipid-related functions of SP-A were clearly correlated with the thermal stability of the collagen domain and the degree of oligomerization. Structural properties and lipid-related characteristics of SP-A1 expressed in mammalian cells but not in insect cells were close to that of natural human SP-A. On the other hand, the lack of glycosylation did not affect either collagen domain stability or conformational changes induced by calcium in the globular domain. However, the lack of glycosylation favored nonspecific thermally induced aggregation of the protein.

Surfactant protein A (SP-A)[1] is a large oligomeric apolipoprotein found primarily in the alveolar fluid of mammalians. SP-A belongs to the collectin (collagen−lectin) family characterized by an NH2-terminal collagen-like domain and a globular COOH-terminal domain that includes a C-type carbohydrate recognition domain (CRD). These proteins, together with the first component of the complement (C1q), are also called defense collagens because they play important roles in innate immunity (*1−3*). SP-A is also involved in the immunomodulation of inflammatory processes of the lung. Unlike other collectins, SP-A is a lipid binding protein, a property that allows this collectin to position and concentrate along with the extracellular membranes that line the alveolar epithelium (*4*). The ability of SP-A to bind lipids is of relevance in several aspects of pulmonary surfactant biology (*1, 4*).

The primary structure of mature SP-A is highly conserved among different mammalians. It consists of four structural domains: (1) an NH2-terminal domain involved in intermolecular disulfide bond formation; (2) a collagen domain, rich in hydroxyproline, important for oligomerization of SP-A; (3) a neck region consisting of amino acid residues with high α-helical properties, involved primarily in protein trimerization; and (4) a globular COOH-terminal domain involved in lipid binding and also in Ca^{2+}-dependent binding of oligosaccharides (*5, 6*). This domain contains two conserved tryptophan residues (located at positions 191 and 213) and a glycosylation site (located at residue Asn[187]). SP-A is modified after translation (cleavage of the signal peptide, proline hydroxylation, and N-linked glycosylation) and assembled into a complex oligomeric structure that resembles a flower bouquet (*7*). In one of the initial steps of the assembly, trimers of SP-A are built up by the association of three polypeptide chains, the collagen regions of which intertwine to form a collagen triple helix that is stabilized by interchain disulfide bonds. In the final stage of the assembly, the octadecamers appear to be formed by lateral association of the NH2-terminal half of six triple-helical stems (*7, 8*).

In humans there are two functional genes (*SP-A1* and *SP-A2*) (*9*) corresponding to two different SP-A cDNA sequences (*10*); however, other mammalian species studied

---

* To whom correspondence should be addressed. Tel: 34-91-3944261. Fax: 34-91-3944672. E-mail: ccasalsc@bio.ucm.es.

[‡] These authors contributed equally to this study.

[§] Complutense University of Madrid.

[ǁ] ALTANA Pharma AG.

[1] Abbreviations: CD, circular dichroic; CHO, Chinese hamster ovary; CRD, carbohydrate recognition domain; DPPC, 1,2-dipalmitoyl-*sn*-glycero-3-phosphocholine; DPPG, 1,2-dipalmitoyl-*sn*-glycero-3-phosphoglycerol; Re-LPS, rough lipopolysaccharide; SP-A, surfactant protein A; AP-SP-A, SP-A isolated from alveolar proteinosis patients; natural hSP-A, SP-A isolated from healthy human donors; SP-A1[hyp], hydroxyproline-deficient recombinant SP-A1 produced in insect cells; SP-A1[hyp,187Ser], glycosylation-deficient mutant SP-A1 produced in insect cells; SP-A1m, recombinant human SP-A1 expressed in CHO cells; T_m, midpoint transition melting temperature.

(except baboons) (*11*) have only one. The nucleotide sequence differences between the two human genes that result in amino acid changes are located in the signal peptide, collagen-like, and globular domains of the resulting proteins (*12*). The major differences between mature SP-A1 and SP-A2 are in the collagen domain (*12*). The importance of proline hydroxylation (in the Y position of the collagen-like Gly-X-Y- region) on the structure of human SP-A has not been previously demonstrated. The first objective of this study was to compare recombinant human SP-A1 expressed in mammalian cells, which is posttranslationally modified by proline hydroxylation and N^{187}-linked glycosylation, with recombinant human SP-A1 from baculovirus-mediated insect cells, which lacks proline hydroxylation. Another feature which is likely to differ between insect cell-derived and mammalian cell-derived human SP-A1 is the Asn^{187}-linked glycosylation. The insect cells do not glycosylate proteins in the same manner as mammalian cells (*13*). Insect cells are unable to add the terminal sialic acid residues found on many mammalian carbohydrate modifications (*13*) and, in particular, in human SP-A (*14*). Thus, our second objective was to determine the structural and functional importance of N^{187}-linked glycosylation. Therefore, we compared the wild-type SP-A1 expressed in insect cells with a nonglyco-sylated variant, in which the Asn at amino acid position 187 was exchanged for a Ser. The comparison of glycosylation-deficient mutant with the wild type will allow the determination of the effect of complete removal of N^{187}-linked sugars on the molecular and functional properties of SP-A1.

In this paper we have studied the structural properties of these recombinant SP-A1 proteins and their lipid-related functions in comparison with those of natural human SP-A from healthy subjects, which likely consists of SP-A1 and SP-A2 molecules. In addition, we have analyzed human SP-A from alveolar proteinosis patients (AP-SP-A) because most of the structural and functional studies reported with human SP-A were performed with AP-SP-A. A complete understanding of the structure and function of human SP-A will allow defining the most appropriate expression system for the production of a recombinant human SP-A form (SP-A1 or SP-A2) to be used in human therapies. The domain structures of the recombinant and mutant proteins used in this study are shown in Figure 1.

EXPERIMENTAL PROCEDURES

Experiments presented in this study were performed with two different preparations of natural human SP-A, one isolated from one healthy donor and another from four different healthy donors; four different preparations of SP-A isolated from four alveolar proteinosis patients (referred to as AP-SP-A); several preparations of SP-A1 ($6A^2$ allele) expressed in either mammalian CHO cells (referred to as SP-A1m) or insect cells (referred to as SP-A1^{hyp}); and a nonglycosylated SP-A1 variant ($6A^2$) also expressed in insect cells (referred to as SP-A1^{hyp,187Ser}) (Figure 1). Experiments were repeated at least twice with each protein preparation.

Cloning and Expression of Recombinant Human SP-A1 Expressed in Mammalian and Insect Cells. The recombinant wild-type form of human SP-A1 ($6A^2$ allele) was expressed in stably transformed CHO cells as described by Voss et al. (*7, 15*) and purified from culture supernatant by mannose
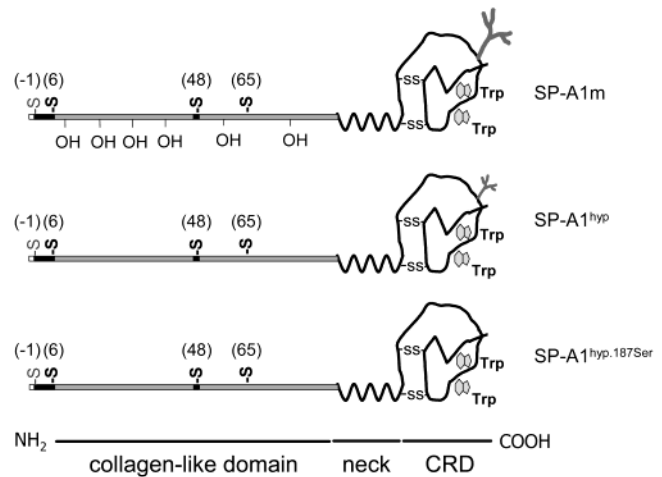

FIGURE 1: Scheme of SP-A. Domain structures of the polypeptide chain of different recombinant forms of SP-A1 are shown. SP-A1m is expressed in CHO cells. SP-A^{hyp} is expressed in insect cells and is deficient in prolyl hydroxylation. SP-A^{hyp,187Ser} is a glycosylation-deficient mutant SP-A1 produced in insect cells. Branched structures represent N-linked carbohydrates. -S denotes cysteine residues at positions -1 and 6 (at the N-terminal segment), 48 (at the Pro-Cys-Pro-Pro interruption between the two collagen-like regions), and 65 (at the triple helix above the interruption) of mature SP-A1.

affinity chromatography. The endotoxin content was 200 pg/mg of SP-A as determined by the LAL clotting test (ENDOSAFE, Charles River).

The cDNA for human SP-A1 ($6A^2$ allele) contained in the plasmid pMTE HS10/5 was subcloned into the *Eco*RI site of the baculovirus expression vector pVL1393. A nonglycosylated variant (N187S), in which the asparagine at amino acid position 187 was exchanged for a serine, was generated by in vitro mutagenesis using the QuickChange mutagenesis kit from Stratagene (Heidelberg, Germany). The oligos used were OZ433 (5′-GACCCCTGTAAGCTACAC-CAACTGG-3′) as sense and OZ434 (5′-CCAGTTGGTG-TAGCTTACAGGGGTC-3′) as antisense primers, respectively. The nucleotide sequences were verified by sequencing (GATC, Konstanz, Germany). Recombinant baculovirus stocks were generated as described in the manufacturer's protocol (Invitrogen, Breda, NL). The SP-As were expressed in SF21 cells using serum-free Insect Express medium (PAA, Marburg, Germany) and purified from the medium by mannose affinity chromatography. The endotoxin content was 56 and 100 pg/mg of SP-A for SP-A1^{hyp} and SP-A1^{hyp,187Ser}, respectively.

Human Lung Tissue Procurement and Isolation of Natural hSP-A. As a source of lung tissue, we used male multiple organ donors. The review board and the ethics committee of the San Carlos Hospital have approved this study. Ages ranged from 19 to 50 years, and cranial trauma or spontaneous intracranial hemorrhage was the cause of death in all of them. Donors with either a recent history of tobacco smoking, more than 72 h of mechanical ventilation, or any radiological pulmonary infiltrate were excluded from this study. Immediately after the left lung was obtained, a bronchoalveolar lavage was performed at 4 °C as previously described (*16*).

SP-A was purified from isolated surfactant using sequential butanol and octyl glucoside extractions (*17*). AP-SP-A was isolated from bronchoalveolar lavages from alveolar proteinosis patients as described above. The purity of SP-A was

checked by one-dimensional SDS−PAGE in 12% polyacrylamide gel under reducing conditions (50 mM dithiothreitol). Quantification of SP-A was carried out by amino acid analysis in a Beckman System 6300 high-performance analyzer. The protein hydrolysis was performed with 0.2 mL of 6 M HCl, containing 0.1% (w/v) phenol, in evacuated and sealed tubes at 108 °C for 24 h. Norleucine was added to each sample as the internal standard (*18*). The endotoxin content of natural human SP-A and AP-SP-A was about 300 pg of endotoxin/mg of SP-A as determined by *Limulus* amebocyte lysate assay (Bio-Whittaker, Walkersville, MD).

Polyacrylamide Gel Electrophoresis under Native Conditions and Silver Staining. The oligomeric assembly of the various SP-As was analyzed by different PAGE techniques. Two micrograms of each protein was subjected to electrophoresis under native conditions. SP-A protein samples were not denatured by chemicals and heating. Electrophoresis was performed at 4 °C with a 7% Tris−acetate PAA gel (NOVEX) in the presence or absence of 4% β-mercaptoethanol. To determine the oligomeric state of SP-A in bands from native gels, bands were excised from nonreduced native gels, incubated with SDS sample buffer, and subjected to electrophoresis on a 12% SDS−PAGE without reducing agents. The molecular mass of the disulfide-linked oligomers was determined by comparison with a molecular mass standard (data not shown). In addition, 2 μg of each of the SP-As was separated on a precasted 4−12% gradient SDS−polyacrylamide gel (NOVEX, Invitrogen, Breda, NL) under denaturing and nonreducing conditions. Purity and apparent molecular masses of monomeric SP-As were determined by 12% SDS−PAGE under reducing conditions. Proteins were visualized by a silver stain as described by Heukeshoven and Dernick (*19*). Prestained SeeBlue (NOVEX) was used as the molecular mass marker.

CD Measurements. CD spectra were obtained on a Jasco J-715 spectropolarimeter fitted with a 150 W xenon lamp (*20−22*). Quartz cells with a 1 mm path length were used, and the spectra were recorded in the far-UV region (190−260 nm) with a scanning speed of 50 nm/min and at the indicated temperature. Four scans were accumulated and averaged for each spectrum. The acquired spectra were corrected by subtracting the appropriate blanks, subjected to noise reduction analysis, and presented as molar ellipticities (deg·cm^2·dmol^{-1}) assuming 110 Da as the average molecular mass per amino acid residue. All measurements were performed in 5 mM Tris-HCl buffer, pH 7.2, and protein concentrations in all cases were 120 μg/mL. The concentration of each SP-A sample was always determined by amino acid analysis.

For the analysis of thermal stability of natural and recombinant human SP-As, melting curves were monitored at 207 nm while the sample temperature was raised from 20 to 65 °C, with an average heating rate of 12 °C/h. SP-A concentrations were 120 μg/mL, and quartz cells with a 1 mm path length were used. The fraction folded was calculated from the equation $F = ([\theta] - [\theta]_u)/([\theta]_n - [\theta]_u)$, where $[\theta]$ is the observed mean residue molar ellipticity at 207 nm and $[\theta]_n$ and $[\theta]_u$ are the mean values for natural and unfolded SP-A, respectively. These values were obtained from the plateau before and after the transition. The temperature where the protein was 50% unfolded ($F = 0.5$) was taken as the melting temperature.

Fluorescence Measurements. Fluorescence experiments were carried out on an SLM-Aminco AB-2 spectrofluorometer as previously described (*18*, *20*). Cells of 10 × 10 mm were used. The slit widths were 4 nm for the excitation and emission beams. The sample was stirred continuously in a sample compartment thermostated with a compact refrigerated circulator, Julabo F30-C. Fluorescence spectra of SP-A were measured at the indicated temperature in 1.6 mL of 5 mM Tris-HCl buffer (pH 7.2). The final protein concentration of SP-A was 10 μg/mL. The blanks and protein samples were excited at 275 nm for measuring the total protein fluorescence spectrum or at 295 nm to preferentially excite tryptophan residues. Emission spectra were recorded from 300 to 400 nm.

The change in fluorescence emission intensity of SP-A upon addition of millimolar concentrations of Ca^{2+} was determined by adding a concentrated solution of CaCl$_2$ to the protein solution in the cuvette (2 mM final concentration). After equilibration for 15 min, the emission spectrum of SP-A was recorded on excitation at 275 nm. Next, the fluorescence spectrum of SP-A was recorded upon addition of 4 mM EDTA. The fluorescence intensity readings were corrected for the dilution caused by aliquot addition. The absorbance of the protein was measured after addition of calcium and EDTA by use of a Beckman DU-640 spectrophotometer.

SP-A Self-Association Assays. Self-association assays of SP-A were performed as previously described (*22*, *23*) by measuring the change in protein absorbance at 360 nm in a Beckman DU-640 spectrophotometer at the indicated temperatures.

Lipid Aggregation Assays. Synthetic phospholipids, DPPC and DPPG, were purchased from Avanti Polar Lipids (Birmingham, AL), and their homogeneity was routinely tested on thin-layer chromatography. Rough LPS from *Salmonella minnesota* (serotype Re-595) was purchased from Sigma Chemical Co. (St. Louis, MO). The organic solvents (methanol and chloroform) used to dissolve lipids were of HPLC grade (Scharlau, Barcelona, Spain).

DPPC/DPPG (7:3) (w/w) vesicles were prepared at a phospholipid concentration of 1 mg/mL by hydrating dry lipid films in a buffer containing 150 mM NaCl, 0.1 mM EDTA, and 5 mM Tris-HCl buffer (pH 7.2) and allowing them to swell for 1 h at 50 °C. Sonication, phosphorus determination, and vesicle size analysis were performed as described previously (*21*). Re-LPS was hydrated for 1 h in 5 mM Tris-HCl buffer (pH 7.2) containing 150 mM NaCl and 0.1 mM EDTA.

LPS aggregation or DPPC/DPPG vesicle aggregation induced by SP-A was studied either at 25 or 37 °C by measuring the change in absorbance at 400 nm in a Beckman DU-640 spectrophotometer. SP-A-induced LPS aggregation assays were performed as described elsewhere (*20*). Briefly, the sample cuvette was first filled with Re-LPS (40 μg/mL final concentration) in 5 mM Tris-HCl buffer (pH 7.2), 150 mM NaCl, and 0.2 mM EDTA. After a 10 min equilibration at 25 °C (or 37 °C), natural or recombinant SP-A (20 μg/mL) was added to the sample cuvette, and the change in optical density at 400 nm was monitored. Next, Ca^{2+} (2.5 mM) was added to both the sample and reference cuvettes, and the change in absorbance was monitored again. Ca^{2+}-dependent LPS aggregation was reversed by adding EDTA
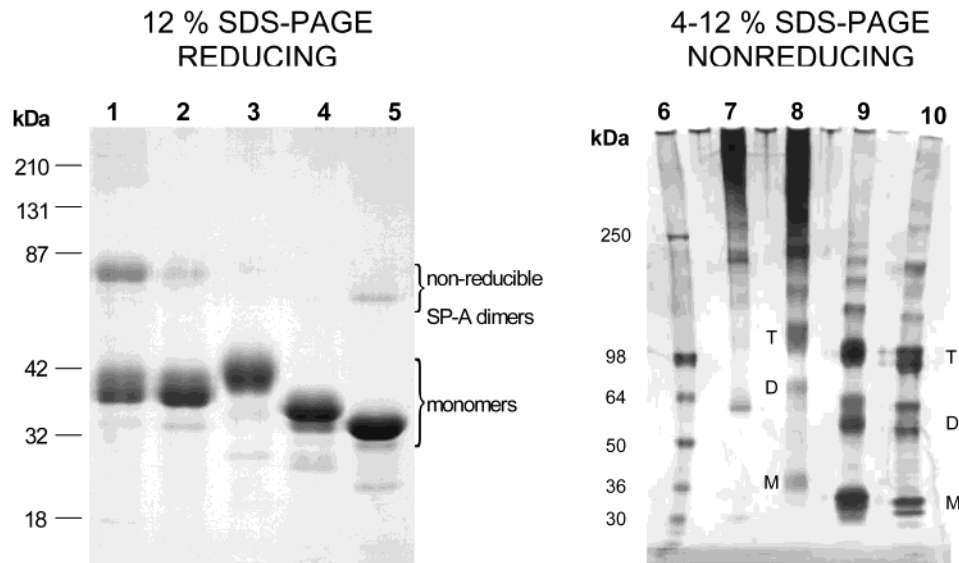
FIGURE 2: Electrophoretic analysis of SP-A. Proteins were subjected to 12% SDS−PAGE under reducing conditions (lanes 1−5) and to 4−12% SDS−PAGE under nonreducing conditions (lanes 6−10) and visualized by silver staining. AP-SP-A (lanes 1 and 7), natural human SP-A (lane 2), SP-A1m (lanes 3 and 8), SP-A1^{hyp} (lanes 4 and 9), and SP-A1^{hyp,187Ser} (lanes 5 and 10) are shown. Lane 6 corresponds to a molecular mass standard (SeeBlue, Novex). Abbreviations: M, monomers; D, dimers; T, trimers.

(5 mM final concentration). The extent of Ca^{2+}-dependent aggregation of Re-LPS in the absence of SP-A was also evaluated.

SP-A-induced phospholipid vesicle aggregation assays were performed as described elsewhere (*20−23*). Recombinant SP-A1s expressed in mammalian or insect cells were assayed at 25 °C at a phospholipid to SP-A weight ratio of 5:1. Assays to compare recombinant SP-A1m with natural human SP-A were performed at 37 °C at a phospholipid to SP-A weight ratio of 10:1. The final concentrations of Ca^{2+} and EDTA were 2 and 4 mM, respectively. The contribution of self-association of SP-A (at a concentration of 20 μg/mL) to the change of absorbance at 400 nm was routinely checked under the experimental conditions in which Re-LPS aggregation or phospholipid vesicle aggregation assays were done.

Adsorption Assay. The ability of lipid extracts of human or porcine surfactants (LES) to adsorb onto and spread at the air−water interface was tested at 25 °C on a Wilhelmy-like highly sensitive surface microbalance, coupled to a small Teflon dish (2.9 × 1.4 cm) as previously reported (*24*). Lipid extracts of surfactants (LES), which contain surfactant lipids, SP-B, and SP-C, were prepared by chloroform/methanol extraction (*16*). Total phospholipid was determined by phosphorus analysis as described by Rouser et al. (*25*). The ability of recombinant SP-A1s to enhance the adsorption of surfactant-like membranes onto an air−liquid interface was studied by addition of recombinant SP-A1 (10 μg/mL) into the hypophase chamber of the Teflon dish, which contained 6 mL of 5 mM Hepes buffer, pH 7.0, 150 mM NaCl, and 5 mM $CaCl_2$. After LES injection (50−100 μg of phospholipids/mL) into the hypophase, phospholipid interfacial adsorption was measured following the change in surface tension as a function of time.

RESULTS

Electrophoretic Characterization. The electrophoretic characterization of natural human SP-A, AP-SP-A, and different recombinant forms of human SP-A1 on SDS−PAGE under reducing conditions is given in Figure 2. AP-SP-A migrated as a monomer (>36 kDa) and as a nonreducible dimer (70 kDa). This electrophoretic pattern was also characteristic of human SP-A from healthy donors, as shown elsewhere (*26*). Recombinant human SP-A1 expressed in either mammalian or insect cells migrated as a monomer on SDS−PAGE under reducing conditions. However, bands with a apparent molecular mass corresponding to a dimer can also be detected. The protein in these electrophoretic bands was identified as SP-A by tryptic digestion and mass spectrometric analysis of the obtained peptides (data not shown). Most of the differences in molecular mass between the reduced recombinant SP-A1 forms are likely related to both the absence of hydroxyproline in SP-A1 from insect cells and the different pattern of glycosylation performed in mammalian or insect cells [lanes 3 (SP-A1m) and 4 (SP-A^{hyp}), respectively] as well as to the absence of N^{187}-linked glycosylation [lane 5 (SP-A^{hyp,187Ser}) compared to lane 4 (SP-A^{hyp})]. Figure 2 also shows the electrophoretic analysis of AP-SP-A and different recombinant forms of SP-A1 on SDS gradient gel electrophoresis under nonreducing conditions. This analysis is predictive for the assembly of disulfide-linked polypeptide chains. The treatment of AP-SP-A with SDS and heat (100 °C) under nonreducing conditions yielded mainly bands corresponding to large oligomers. Similar results were found with natural hSP-A (data not shown). Like natural hSP-A, SP-A1m consisted mainly of large oligomeric structures. However, the degree of disulfide-linked structures was less than that of natural hSP-A or AP-SP-A, as demonstrated by the presence of trimeric forms and faint bands corresponding to dimers and monomers. In contrast, SP-As derived from insect cells (both SP-A1^{hyp} and SP-A^{hyp,187Ser}) differ greatly in oligomeric composition from natural hSP-A or SP-A1m, since they consisted of major bands with an electrophoretic mobility corresponding to monomers, dimers, and trimers. The significance of the appearance of two bands for each of these forms is unknown.
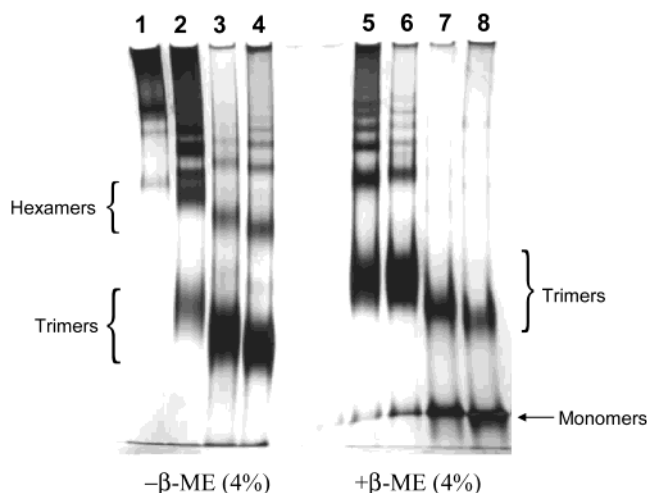
FIGURE 3: Patterns of oligomerization of SP-A under native conditions. Samples (2 μg of each SP-A preparation) were subjected to 7% PAGE under native conditions, in the absence (lanes 1−4) and presence (lanes 5−8) of 4% β-mercaptoethanol, and visualized by silver staining. The arrows indicate bands corresponding to monomers, trimers, or hexamers, determined as indicated in Experimental Procedures. AP-SP-A (lanes 1 and 5), SP-A1m (lanes 2 and 6), SP-A1^{hyp} (lanes 3 and 7), and SP-A1^{hyp,187Ser} (lanes 4 and 8) are shown.

On the other hand, the presence of bands corresponding to dimers and monomers in nonhydroxylated SP-A1s derived from insect cells (SP-A1^{hyp} and SP-A^{hyp,187Ser}) suggests that, at least in part of these molecules, only two polypeptide chains of the triple helix are covalently linked by disulfide bonds. In contrast, in the case of AP-SP-A and SP-A1m, at least two cysteine residues (likely Cys^6 and Cys^{48}) cross-link the three polypeptide chains of the triple helix.

The relative extent of oligomerization of recombinant human SP-A1 produced in mammalian and insect cells was examined by electrophoresis under native conditions (Figure 3). SP-A molecules maintain their natural conformation because they were not treated with SDS, with reducing agents, or with heat. Figure 3 shows that AP-SP-A (lane 1) consisted primarily of octadecamers. Similar data were found for human SP-A from healthy subjects (*20*). SP-A1m (lane 2) was composed of a mixture of oligomers (tri-, hexa-, nona-, dodeca-, and octadecamers), whereas SP-A1^{hyp} and SP-A^{hyp,187Ser} (lanes 3 and 4, respectively) consisted primarily of trimers with smaller amounts of hexamers or larger oligomeric forms. Figure 3 also shows the electrophoretic analysis under native (no SDS and no heat) but reducing conditions. The presence of reducing agents yielded mainly trimers but not the monomeric form for AP-SP-A and SP-A1m (lanes 5 and 6, respectively), indicating that trimers can be formed independently of disulfide bridges. Additionally, oligomers larger than trimers were also visualized, mainly in AP-SP-A, indicating that noncovalent interactions are also involved in the formation of hexamers and larger oligomeric forms. In contrast, the presence of reducing agents yielded only monomers and trimers from nonhydroxylated SP-A1 derived from insect cells (either glycosylated or nonglycosylated, lanes 7 and 8, respectively). These data suggest that the trimeric stems of nonhydroxylated SP-A1 are less stable without disulfide bridges.

Circular Dichroic Spectra and Thermal Stability. Circular dichroic (CD) spectroscopy was used to examine the thermal

stability of the collagen domain. Figure 4 compares the CD spectra of AP-SP-A and natural human SP-A with those of different recombinant human SP-A1s (SP-A1m, SP-A1^{hyp}, and SP-A^{hyp,187Ser}) at 20 and 70 °C. Previous evidence using CD spectroscopy showed that natural human SP-A isolated by butanol extraction is characterized by a strong negative extreme at 207 nm and a shoulder at 223 nm (*20*), also reported for canine, porcine, or alveolar proteinosis human SP-A (*18, 21, 22, 27, 28*). Figure 4 shows that all recombinant forms of SP-A1, expressed in mammalian or insect cells (either glycosylated or nonglycosylated), displayed a shape similar to that of natural hSP-A at 20 °C, indicating similar secondary structure. These results are in agreement with those reported recently for recombinant SP-A1, SP-A2, and coexpressed SP-A1/SP-A2 produced in insect cells (*20*). Figure 4 also shows that heat treatment of natural hSP-A, AP-SP-A, and different recombinant forms of SP-A1 at 70 °C resulted in a pronounced decrease in the magnitude of the negative band at 207 nm, with a blue shift of the minimum in the case of recombinant proteins but not for natural hSP-A or AP-SP-A. We recently demonstrated that the change in ellipticity during the transition from 20 to 70 °C can be fitted to a structural transition between two components, which closely follows the denaturation profile of collagen (*22*). This suggests that there is no additional contribution of changes affecting other structural components in that range of temperature.

The thermal denaturation of the collagen domain of different recombinant forms of SP-A1 is shown in Figure 5 along with that of natural hSP-A, which has been reported recently (*20*). The midpoint melting temperature of these proteins, including that of AP-SP-A, is given in Table 1. Midpoint melting temperatures of recombinant SP-A1 expressed in insect cells (either glycosylated or nonglycosylated) were reduced by about 9 °C with respect to that of recombinant SP-A1 expressed in mammalian cells. These data indicate that the T_m of SP-A1 depends on the hydroxylation of proline residues. Glycosylation in Asn^{187} does not seem to have any influence on T_m. On the other hand, the lower T_m of recombinant human SP-A1 expressed in mammalian cells (44.5 ± 0.35) with respect to natural human SP-A (48 ± 0.05) might be related to the lower proportion of octadecameric structures relative to the proportion of inferior size forms (pentadecamers, dodecamers, hexamers, and trimers). The T_m of AP-SP-A calculated in this study from protein preparations isolated from four different patients was lower than that reported elsewhere (*28*). This is likely a consequence of variation among individuals (from 42.8 to 50 °C).

Fluorescence Characteristics. The fluorescence of SP-A is dominated by the contribution of its two conserved tryptophan residues, which are located at positions 191 and 213 in human SP-A and all species studied until now. These two tryptophans are located near the calcium binding site located in the center of the sugar binding site. Therefore, they are sensitive markers of conformational changes in this region. Figure 6 shows that the fluorescence emission spectrum of natural hSP-A and different recombinant forms of human SP-A1 on excitation at 275 was characterized by a fluorescence emission maximum at about 330 nm. Addition of 2 mM Ca^{2+} led to a blue shift in the wavelength of the emission maximum from 330 to 326 nm, indicating that the
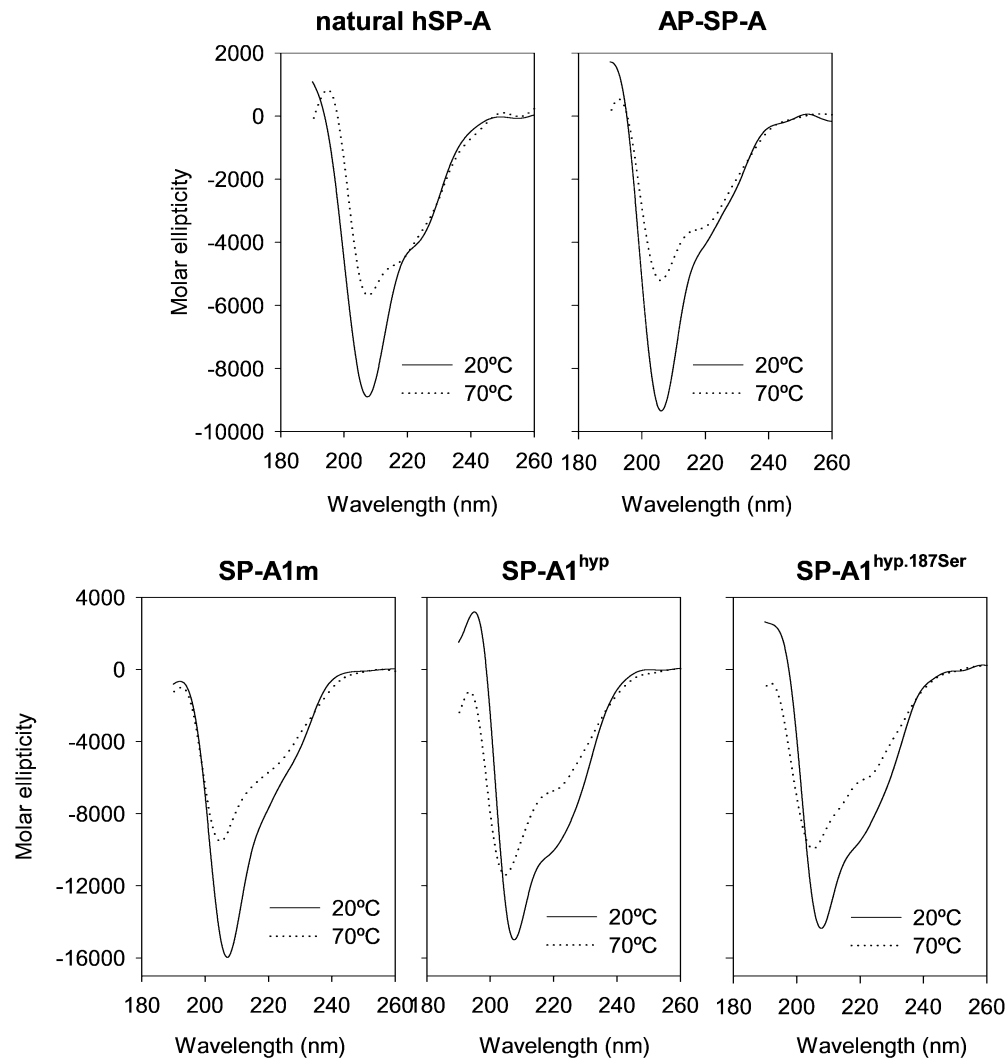
FIGURE 4: Circular dichroic spectra of natural human SP-A, AP-SP-A, and different recombinant forms of SP-A1 at 20 and 70 °C. All measurements were performed in 5 mM Tris-HCl buffer, pH 7.2. Protein concentrations in all cases were 120 μg/mL, as determined by amino acid analysis.
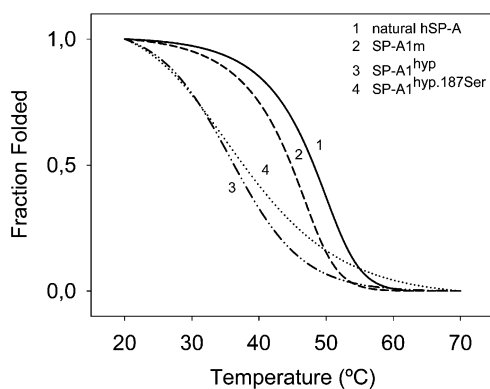

FIGURE 5: Unfolding curves of natural human SP-A and different recombinant forms of SP-A1. Melting curves were monitored at 207 nm, at 120 μg of SP-A/mL, while the sample temperature was raised from 20 to 70 °C (12 °C/h). The fraction folded (*F*) was calculated from the equation $F = ([\theta] - [\theta]_u)/([\theta]_n - [\theta]_u)$, where $[\theta]$ is the observed mean residue molar ellipticity at 207 nm, while $[\theta]_n$ and $[\theta]_u$ are the mean values for natural and unfolded SP-A, respectively.

binding of calcium led to a conformational change in the protein, affecting the polarity in the environment of the tryptophan residues. Chelating calcium with EDTA reversed

Table 1: Midpoint Transition Melting Temperature of Human SP-A[a]

protein	T_m (°C)
SP-A1[hyp]	36.2 ± 0.01
SP-A1[hyp,187Ser]	37.4 ± 1.2
SP-A1m	44.5 ± 0.35
natural hSP-A[b] (*n* = 2)	48.0 ± 0.05
AP-SP-A[b] (*n* = 4)	46.2 ± 3.1

[a] Values are expressed as the mean ± the standard deviation of three experiments. [b] Data are expressed as the mean ± the standard deviation of different preparations of SP-A from different individuals.

the spectral changes induced by calcium, causing a red shift in the fluorescence emission maximum (from 326 to 330 nm). These results are consistent with previous results obtained with recombinant SP-A1[hyp] preparations produced elsewhere (*20*). Figure 6 also shows intrinsic fluorescence characteristics of natural human SP-A and recombinant forms of SP-A1 in the absence or presence of calcium, at a temperature (70 °C) in which the collagen-like domain of all these proteins was denatured. All different recombinant forms of SP-A1 and natural hSP-A heated at 70 °C showed a similar position of the fluorescence emission maximum of tryptophan residues and similar spectral changes with calcium
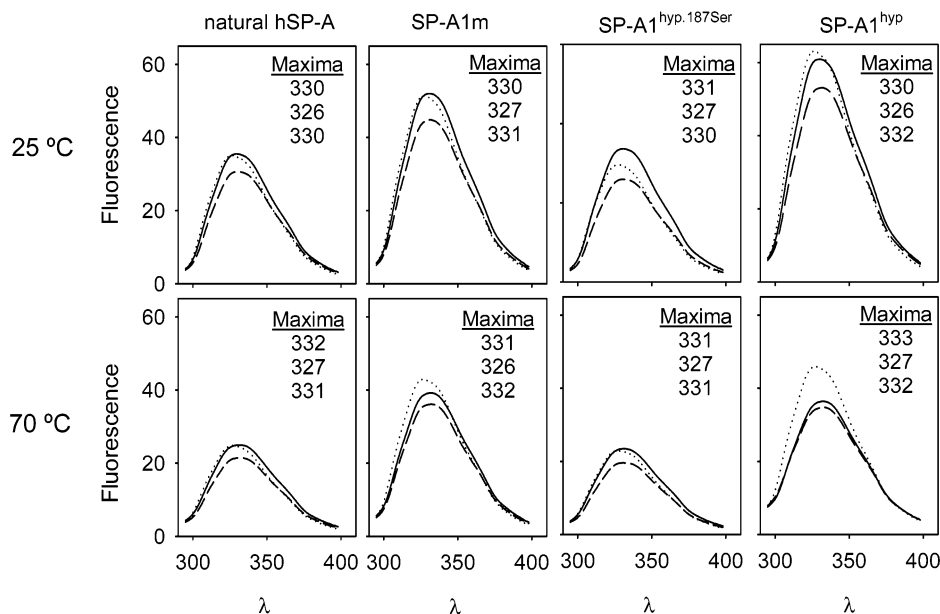
FIGURE 6: Fluorescence emission spectra of natural human SP-A and different recombinant forms of SP-A1 at 25 and 70 °C. The solid lines represent the emission spectra on excitation at 275 nm in 5 mM Tris-HCl buffer (pH 7.2). The dotted lines correspond to repeat emission spectra 10 min after the addition of Ca^{2+} to a final concentration of 2 mM. The dash−dot lines represent repeat emission spectra 10 min after the addition of EDTA (4 mM final concentration). Values of the emission maxima of SP-A under different conditions are given in the following order: (1) 5 mM Tris-HCl buffer (pH 7.2); (2) after addition of Ca^{2+}; (3) after addition of EDTA.
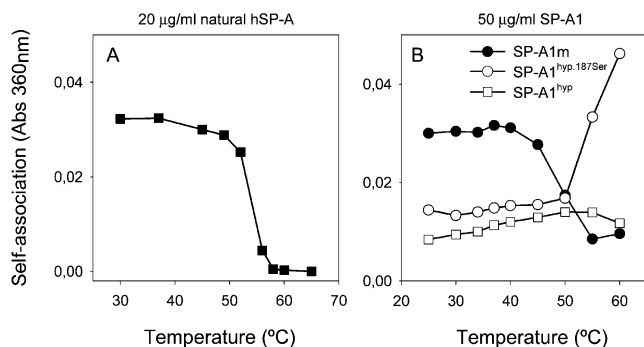

FIGURE 7: Ca^{2+}-dependent self-association of natural human SP-A (A) and different recombinant forms of SP-A1 (B) as a function of temperature. Natural hSP-A (20 μg/mL) and different recombinant forms of SP-A1 (50 μg/mL) were added to the sample cuvette filled with 5 mM Tris-HCl buffer (pH 7.2). The turbidity change at 360 nm was monitored at the indicated temperatures at 1 min intervals. After stabilization, 5 mM Ca^{2+} (final concentration) was added to both the sample and reference cuvette, and the turbidity changes were monitored again at 1 min intervals until the absorbance was stabilized. From the kinetics of Ca^{2+}-induced self-association of SP-A at different temperatures, the extent of SP-A self-association at each temperature was determined.

and EDTA. This indicates a remarkable thermal stability of the globular domain of SP-A in which the tryptophan residues are located. Moreover, calcium-induced conformational changes in the surroundings of SP-A aromatic side chains were not affected by unfolding of the collagen-like domain. On the other hand, Figure 6 also shows that the lack of glycosylation in Asn^{187} had little influence on the fluorescence characteristics of SP-A1[hyp,187Ser]. The decrease in fluorescence intensity of the glycosylation-deficient mutant in comparison with SP-A1[hyp] might be a consequence of the tendency of this mutant to self-aggregate (see Figure 7). Self-aggregation can affect fluorescence characteristics of SP-A (22).

Effect of Temperature on Self-Association of Different Recombinant Forms of SP-A1. Figure 7A shows that Ca^{2+}-dependent self-association activity of natural human SP-A is completely inhibited by unfolding of the collagen-like domain, supporting previous results with porcine SP-A (22). Figure 7B shows the effect of temperature on self-association activity of recombinant human SP-A1 expressed in mammalian or insect cells. Similar to natural human SP-A, the ability of recombinant SP-A1m to undergo self-association in the presence of calcium required a structurally intact collagen domain (Figure 7B). In contrast, SP-A1[hyp] hardly self-associated at any temperature. The lack of self-association activity in SP-A1[hyp] supports recently reported results with SP-A1 expressed in insect cells (20). In addition, it suggests that the oligomeric status of the protein, which seems to be correlated with proline hydroxylation in the collagen domain, must play a major role in the self-association process. On the other hand, the glycosylation-deficient mutant (SP-A1[hyp,187Ser]) seemed to suffer nonspecific thermally induced aggregation, which may be responsible for rapid increase in signal at high temperature (Figure 7B).

Lipid-Related Functions of Different Recombinant Forms of SP-A1. The assessment of Ca^{2+}-dependent LPS aggregation induced by different recombinant forms of SP-A1 and natural human SP-A is shown in Figure 8. We recently found that SP-A-induced LPS aggregation was inhibited by unfolding of the collagen-like domain (20). Therefore, these experiments were done at 25 °C, a temperature lower than the T_m for the collagen domain of all these recombinant proteins. Figure 8 shows that rough LPS aggregates in buffers containing calcium and that only natural human SP-A and SP-A1m were able to foster further aggregation of the rough LPS. SP-A1m-induced LPS aggregation was lower than that induced by natural human SP-A. SP-A1[hyp] or SP-A1[hyp,187Ser] decreased the rate of rough LPS aggregation induced by calcium in the absence of any protein, indicating that these
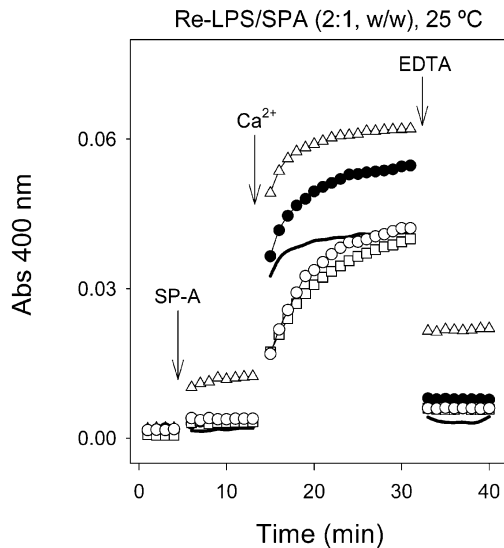
FIGURE 8: Re-LPS aggregation induced by natural human SP-A and different recombinant forms of SP-A1. The sample cuvette was first filled with Re-LPS (40 μg/mL final concentration) in 5 mM Tris-HCl, 150 mM NaCl, and 0.1 mM EDTA buffer at pH 7.2. After a 10 min equilibration at 25 °C, SP-A (20 μg/mL) was added to the sample cuvette, and the change in optical density at 400 nm was monitored. Next, 2.5 mM Ca^{2+} was added to the sample and reference cuvettes, and the change in absorbance was monitored again. Ca^{2+}-dependent Re-LPS aggregation was reversed by addition of EDTA (5 mM). Natural hSP-A (open triangles), SP-A1m (closed circles), SP-A1[hyp] (gray squares), and SP-A1[hyp,187Ser] (open circles) are shown. Ca^{2+}-dependent Re-LPS aggregation in the absence of SP-A is also shown (solid line).
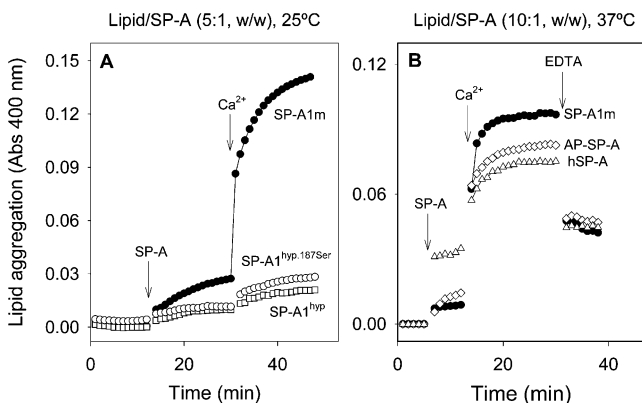

FIGURE 9: Vesicle aggregation induced by SP-A. Panel A: DPPC/DPPG vesicle aggregation induced by different recombinant forms of SP-A1 at 25 °C and at a lipid:SP-A weight ratio of 5:1 (100 μg of phospholipids/mL and 20 μg of SP-A/mL). Panel B: Comparison of vesicle aggregation activity of SP-A1m with that of AP-SP-A and natural human SP-A at 37 °C and at a lipid:SP-A weight ratio of 10:1 (50 μg of phospholipids/mL and 5 μg of SP-A/mL). Natural hSP-A (open triangles), AP-SP-A (open diamonds), SP-A1m (closed circles), SP-A1[hyp] (gray squares), and SP-A1[hyp,187Ser] (open circles) are shown.

nonhydroxylated proteins could bind but not aggregate rough LPS.

Figure 9A compares the ability of different recombinant forms of SP-A1 to induce DPPC/DPPG vesicle aggregation in the presence of calcium at a temperature (25 °C) lower than the T_m for the collagen domain of these recombinant proteins. The capability of hydroxylated SP-A1m to aggregate phospholipid vesicles was much higher than those of nonhydroxylated SP-A1[hyp] or SP-A1[hyp,187Ser]. These results indicate that the presence of hydroxyproline is also important
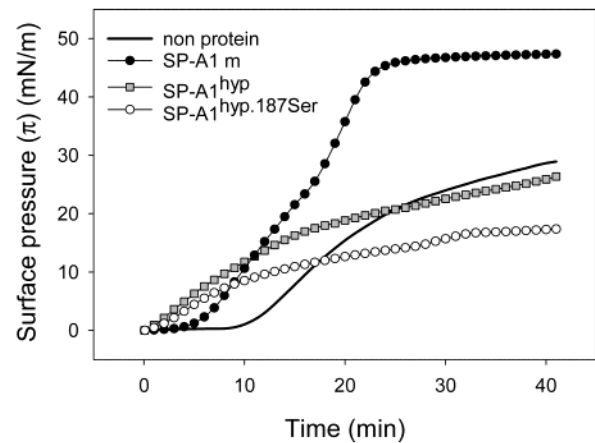

FIGURE 10: Effect of different recombinant forms of SP-A1 on the adsorption kinetics of surfactant-like membranes. Phospholipid interfacial adsorption was measured at 25 °C following the change in surface pressure as a function of time for samples containing 70 μg of phospholipids/mL (surfactant lipid extract, containing SP-B and SP-C) with or without SP-A1 (10 μg/mL) in a final volume of 6 mL of 5 mM Hepes buffer, pH 7.0, 150 mM NaCl, and 5 mM $CaCl_2$.

for phospholipid vesicle aggregation. Figure 9B compares the ability of natural human SP-A, AP-SP-A, and recombinant SP-A1m to induce lipid aggregation. These experiments were performed at 37 °C and at higher lipid:SP-A weight ratio (10:1), conditions close to those present in the alveolar fluid. Results indicated that the capacity of SP-A1m to aggregate lipid vesicles was similar to that of natural hSP-A or AP-SP-A.

Figure 10 shows the curves of surface pressure against time of surfactant-like membranes (containing SP-B and SP-C) in the absence and presence of SP-A1. In the absence of SP-A the curves were sigmoidal, showing a lag time of about 10 min for the concentration of phospholipids used. According to Putman et al. (*29*), the lag time likely represents the rate of transport of phospholipids through the bulk liquid. During this time an increase of surface pressure is absent. The parameter defined as adsorption rate (the tangent to the curve at its point of inflection) likely represents the process of spreading. The equilibrium surface pressure (47 mN/m) was reached at longer times for the concentration of phospholipid used.

The presence of hydroxylated SP-A1m highly enhanced the adsorption rate of surfactant-like membranes from a subphase into an air−water interface and decreased the lag time. Thus, the equilibrium surface pressure (47 mN/m) was reached at shorter times. The competence of SP-A1m to enhance the adsorption rate of human surfactant-like membranes was similar to that of natural hSP-A or AP-SP-A (data not shown). In contrast, the presence of nonhydroxylated SP-A1[hyp] and SP-A1[hyp,187Ser] highly reduced the lag time but decreased the adsorption rate of surfactant-like membranes. These results suggest that these proteins may bind surfactant vesicles and increase the rate of transport of phospholipids through the bulk liquid but do not promote the spreading of the material along the surface.

DISCUSSION

In this study we investigated the effects of proline hydroxylation and Asn[187]-linked glycosylation on the mo-

lecular and functional properties of recombinant human SP-A1. The production of this recombinant protein in mammalian and insect cells presents a unique opportunity to explore the role of proline hydroxylation, since insect cells lack prolyl 4-hydroxylase activity (30–32). The role of the N^{187}-linked oligosaccharide moiety of SP-A was determined by production of a glycosylation-deficient mutant SP-A1 expressed in insect cells, in which Asn^{187} was substituted for Ser to prevent N^{187}-linked oligosaccharide attachment. All of these proteins, schematized in Figure 1, were structurally characterized with respect to covalent and noncovalent oligomerization under native conditions, arrangement of disulfide bonding, secondary structure, thermal stability of the collagen domain, conformational changes in the globular domain identified by intrinsic fluorescence, and ability to self-associate. In addition, the role of hydroxylation and glycosylation on lipid-related functions of SP-A was determined.

Hydroxylation of proline residues in SP-A1m raised the melting temperature of the collagen-like domain by about 9 °C. The T_m values determined by CD analysis were 44.5 °C for SP-A1m expressed in mammalian cells and 36 °C for SP-A1^{hyp} expressed in insect cells. This value is slightly below body temperature. The collagen-like domain of both natural human SP-A (20) and C1q (33) has a T_m of 48 °C, which is well above body temperature. The lower T_m of recombinant human SP-A1 expressed in mammalian cells with respect to natural human SP-A is likely related to the lower proportion of octadecameric structures relative to the proportion of smaller forms. The combination of both gene products (SP-A1 and SP-A2) may be important for the formation of octadecameric tissue SP-A (20).

McCormack et al. reported that hydroxylation of proline residues is required for the formation of octadecamers in rat SP-A (30). Consistent with these findings, our results indicate that the presence of hydroxyproline imparts stability to the triple helical trimers, which in turn may promote lateral association of SP-A trimers to form the microfibril end piece below the kink. First, the electrophoretic analysis of SP-A1 under native conditions in the absence of β-mercaptoethanol indicated that hydroxylated SP-A1m consisted mainly of high oligomeric forms with smaller amounts of trimers, whereas nonhydroxylated SP-A1^{hyp} consisted mainly of trimers with smaller amounts of hexamers. These results suggest that the higher stability of hydroxylated trimeric stems likely promotes lateral association of SP-A trimers to form oligomeric SP-A. Second, the electrophoretic analysis of different recombinant forms of SP-A1 under native conditions in the presence of β-mercaptoethanol indicated that the triple helix of SP-A1m remained intact when disulfide bonds were reduced at low temperatures. Moreover, larger forms of SP-A1m were also visualized, indicating that lateral association of the microfibril end can also be stabilized by noncovalent interactions. By contrast, the treatment of SP-A1^{hyp} with reducing agents at low temperatures yielded the monomeric form, indicating that the trimeric stems of nonhydroxylated SP-A1^{hyp} are less stable and dependent on covalent interaction.

Hydroxylation of proline residues may also influence the arrangement of disulfide bonding on human SP-A1, as suggested for rat SP-A (30). The pattern of disulfide bonds of human SP-A is not clear. Two cysteine residues, one present in the N-terminal segment (Cys^6) and a second cysteine present in the middle of the collagen-like sequence within the Pro-Cys-Pro-Pro interruption (Cys^{48}), are potentially involved in the arrangement of the disulfide bonding (14) (Figure 1). In the rat, the Cys^{-1} disulfide bridge is involved in the formation of rat SP-A oligomers (34, 35). Alveolar proteinosis SP-A also contains the Cys^{-1} isoform (14). N-Terminal sequence analysis of SP-A1 indicated that 60% of recombinant SP-A1^{hyp} and 45% of SP-A1m molecules contain the Cys^{-1} isoform (data not shown). However, the potential implication of this Cys^{-1} residue on the disulfide-bridged structure of human SP-A remains elusive. Likewise, the potential participation of Cys^{65}, located in the collagen domain above the kink (Figure 1), is still undefined. Our results indicate that, at least in some SP-A1^{hyp} molecules, only two polypeptide chains of the triple helix are covalently bound by one or two disulfide bonds because the treatment of this protein with denaturing agents (SDS and heat) under nonreducing conditions yielded dimers and monomers. In contrast, hydroxylated SP-A1m yielded mainly trimers and larger forms, indicating that, in most SP-A1m molecules, two disulfide bonds cross-link the three polypeptide chains of the triple helix, and they must be involved in triple helix and oligomer stabilization. Collectively, these data suggest that the lack of hydroxyproline results in local structural perturbation in the triple helix that affects the arrangement of intermolecular disulfide bonds.

On the other hand, our results demonstrate that the stability of the collagen-like domain, which is linked to proline hydroxylation and the degree of oligomerization, is correlated with the ability of SP-A to self-associate in the presence of calcium. Hydroxylated SP-A1m self-associated at temperatures lower than the T_m for its collagen-like domain (44.5 °C). This behavior is similar to that of natural human SP-A, which self-associated at temperatures lower than 48 °C. Self-association activity of natural human SP-A or SP-A1m was completely inhibited by unfolding of the collagen-like domain, supporting previous results with porcine SP-A (22). In contrast, nonhydroxylated SP-A^{hyp} hardly self-associated at any temperature assayed. SP-A self-association depends on calcium, and Ca^{2+} induces a conformational change in the globular domain of the protein identified by intrinsic fluorescence. Thus, it is possible that specific SP-A–SP-A association occurs among globular heads. A structurally intact collagen domain would ensure the grouping and orientation of globular heads in the oligomer.

One of the most interesting effects of SP-A on surfactant-like phospholipid vesicles is its ability to induce rapid aggregation of these vesicles with or without surfactant hydrophobic proteins SP-B and SP-C (17, 18, 21, 23). This process is dependent on calcium and predicts the surface-active properties of the protein in concerted action with SP-B (17, 36). In addition, SP-A is able to induce aggregation of rough LPS (37). This activity facilitates phagocytosis of endotoxin aggregates by alveolar macrophages and prevents adherence of endotoxins or bacteria to the alveolar epithelium. It is possible that the process of lipid and rough LPS aggregation mediated by SP-A is correlated with that of self-association of the protein. Our results indicate that hydroxylated SP-A1m, but not nonhydroxylated SP-A1^{hyp}, was able to foster rough LPS aggregation in the presence of calcium and to induce phospholipid vesicle aggregation and enhance the adsorption rate of surfactant-like membranes, containing

SP-B and SP-C, to an air−liquid interface. These lipid-related activities might correlate with the ability of SP-A1m, but not SP-A1[hyp], to self-associate in the presence of calcium. The stability of the collagen-like domain and the degree of oligomerization seem to be important in all of these processes.

The structural and functional role of the covalently N[187]-linked complex oligosaccharides of SP-A is yet undefined. The nature of the glycan moiety in AP-SP-A was analyzed in detail by sequential digestions with endoglycosidases and mass spectrometry (*14*). The dominant glycan variant in AP-SP-A is a triantennary complex glycan with a fucose unit linked to the core. However, a large proportion of penta-, tetra-, and diantennary structures are also present. All structures are partially capped with sialic acid residues. Insect cells glycosylate proteins in a simple mannose-rich manner, and they are unable to add the terminal sialic acid residues (*13*). Thus, it is conceivable that recombinant SP-A1[hyp] expressed in insect cells have glycan structures different from those present in natural human SP-A, AP-SP-A, or recombinant SP-A1m expressed in mammalian cells. Consequently, the comparison of the glycosylation-deficient mutant (SP-A1[hyp,187Ser]) with the wild type (SP-A1[hyp]) will allow the determination of the potential contribution of a glycan structure in SP-A1m and SP-A1[hyp] to the structural and functional differences reported above. Our results indicate that the lack of N[187]-linked glycosylation did not affect the secondary structure of the protein, the collagen stability, the physical−chemical environment of tryptophan residues in the globular domain, and conformational changes induced by calcium identified by intrinsic fluorescence. However, the lack of N[187]-linked glycosylation favored nonspecific protein aggregation, which increased with temperature. Nonglycosylated SP-A1[hyp,187Ser] might form nonspecific aggregates at high temperature, when its collagen domain is unfolded. Such nonspecific thermally induced aggregation of SP-A1[hyp,187Ser] seems to be different from Ca^{2+}-dependent self-association of SP-A1m, which depended on a structurally intact collagen-like domain. The oligosaccharide moiety could be an important structural determinant in ensuring accurate self-association of human SP-A and, perhaps, proper interaction with other ligands. In addition, the oligosaccharide moiety of SP-A is apparently necessary for the opsonization of certain viruses, which involves binding of influenza A virus (*38*, *39*) and herpex simplex virus (*40*) to complex oligosaccharides on SP-A. In summary, the data presented here indicate that, for therapeutic purposes, SP-A produced in insect cells may not be a good expression system for the whole molecule. In particular, nonglycosylated SP-A1[hyp,187Ser] would not be a good candidate for therapeutic use due to its marked tendency to nonspecific self-aggregation, its lack of capacity to aggregate LPS, and its decreased ability to aggregate lipids and enhance the adsorption rate of surfactant-like membranes.

ACKNOWLEDGMENT

REFERENCES

1. McCormack, F. X., and Whitsett, J. A. (2002) The pulmonary collectins, SP-A and SP-D, orchestrate innate immunity in the lung, *J. Clin. Invest. 109*, 707−712.
2. Crouch, E., and Wright, J. R. (2001) Surfactant proteins A and D and pulmonary host defense, *Annu. Rev. Physiol. 63*, 521−554.
3. Lu, J., The, C., Kishore, U., and Reid, K. B. (2002) Collectins and ficolins: sugar pattern recognition molecules of the mammalian innate immune system, *Biochim. Biophys. Acta 1572*, 387−400.
4. Casals, C. (2001) Role of surfactant protein A (SP-A)/lipid interactions for SP-A functions in the lung, *Pediatr. Pathol. Mol. Med. 20*, 249−268.
5. McCormack, F. X. (1998) Structure, processing and properties of surfactant protein A, *Biochim. Biophys. Acta 19*, 2−3.
6. Palaniyar, N., Ikegami, M., Korfhagen, T., Whitsett, J., and McCormack, F. X. (2001) Domains of surfactant protein A that affect protein oligomerization, lipid structure and surface tension, *Comp. Biochem. Physiol., Part A: Mol. Integr. Physiol. 129*, 109−127.
7. Voss, T., Eistetter, H., Schafer, K. P., and Engel, J. (1988) Macromolecular organization of natural and recombinant lung surfactant protein SP 28−36. Structural homology with the complement factor C1q, *J. Mol. Biol. 201*, 219−227.
8. Haas, C., Voss, T., and Engel, J. (1991) Assembly and disulfide rearrangement of recombinant surfactant protein A in vitro, *Eur. J. Biochem. 197*, 799−803.
9. White, R. T., Damm, D., Miller, J., Spratt, K., Schilling, J., Hawgood, S., Benson, B., and Cordell, B. (1985) Isolation and characterization of the human pulmonary surfactant apoprotein gene, *Nature 317*, 361−363.
10. Floros, J., Steinbrink, R., Jacobs, K., Phelps, D., Kriz, R., Recny, M., Sultzman, L., Jones, S., Taeusch, H. W., Frank, H. A., et al. (1986) Isolation and characterization of cDNA clones for the 35-kDa pulmonary surfactant-associated protein, *J. Biol. Chem. 261*, 9029−9033.
11. Gao, E., Wang, Y., McCormick, S. M., Li, J., Seidner, S. R., and Mendelson, C. R. (1996) Characterization of two baboon surfactant protein A genes, *Am. J. Physiol. 271*, L617−L630.
12. Floros, J., and Hoover, R. R. (1998) Genetics of the hydrophilic surfactant proteins A and D, *Biochim. Biophys. Acta 1408*, 312−322.
13. Marchal, I., Jarvis, D. L., Cacan, R., and Verbert, A. (2001) Glycoproteins from insect cells: sialylated or not?, *Biol. Chem. 382*, 151−159.
14. Berg, T., Leth-Larsen, R., Holmskov, U., and Hojrup, P. (2000) Structural characterization of human proteinosis surfactant protein A, *Biochim. Biophys. Acta 1543*, 159−173.
15. Voss, T., Melchers, K., Scheirle, G., and Schafer, K. P. (1991) Structural comparison of recombinant pulmonary surfactant protein SP-A derived from two human coding sequences: implications for the chain composition of natural human SP-A, *Am. J. Respir. Cell. Mol. Biol. 4*, 88−94.
16. Casals, C., Herrera, L., Miguel, E., Garcia-Barreno, P., and Municio, A. M. (1989) Comparison between intra- and extracellular surfactant in respiratory distress induced by oleic acid, *Biochim. Biophys. Acta 1003*, 201−203.
17. Hawgood, S., Benson, B. J., Schilling, J., Damm, D., Clements, J. A., and White, R. T. (1987) Nucleotide and amino acid sequences of pulmonary surfactant protein SP 18 and evidence for cooperation between SP 18 and SP 28-36 in surfactant lipid adsorption, *Proc. Natl. Acad. Sci. U.S.A. 84*, 66−70.
18. Casals, C., Miguel, E., and Perez-Gil, J. (1993) Tryptophan fluorescence study on the interaction of pulmonary surfactant protein A with phospholipid vesicles, *Biochem. J. 296*, 585−593.
19. Heukeshoven, J., and Dernick, R. (1988) Improved silver staining procedure for fast staining in PhastSystem Development Unit. I. Staining of sodium dodecyl sulfate gels, *Electrophoresis 9*, 28−32.
20. García-Verdugo, I., Guirong, G., Floros, J., and Casals, C. (2002) Structural analysis and lipid binding properties of recombinant human surfactant protein A (SP-A) derived from one (SP-A1 or SP-A2) or both genes, *Biochemistry 41*, 14041−14053.

21. Ruano, M. L., Perez-Gil, J., and Casals, C. (1998) Effect of acidic pH on the structure and lipid binding properties of porcine surfactant protein A. Potential role of acidification along its exocytic pathway, *J. Biol. Chem. 273*, 15183−15191.

22. Ruano, M. L., Garcia-Verdugo, I., Miguel, E., Perez-Gil, J., and Casals, C. (2000) Self-aggregation of surfactant protein A, *Biochemistry 39*, 6529−6537.

23. Ruano, M. L., Miguel, E., Perez-Gil, J., and Casals, C. (1996) Comparison of lipid aggregation and self-aggregation activities of pulmonary surfactant-associated protein A, *Biochem. J. 313*, 683−689.

24. Casals, C., Varela, A., Ruano, M. L., Valino, F., Perez-Gil, J., Torre, N., Jorge, E., Tendillo, F., and Castillo-Olivares, J. L. (1998) Increase of C-reactive protein and decrease of surfactant protein A in surfactant after lung transplantation, *Am. J. Respir. Crit. Care Med. 157*, 43−49.

25. Rouser, G., Freischer, S., and Yamamoto, A. (1970) Two-dimensional thin layer chromatographic separation of polar lipids and determination of phospholipids by phosphorus analysis of spots, *Lipids 5*, 494−496.

26. Casals, C., Arias-Díaz, J., Valiño, F., Sáenz, A., García, C., Balibrea, J. L., and Vara, E. (2003) Surfactant strengthens the inhibitory effect of C-reactive protein on human lung macrophage-cytokine release, *Am. J. Physiol. Lung Cell. Mol. Physiol. 284*, L466−L472.

27. King, R. J., Simon, D., and Horowitz, P. M. (1989) Aspects of secondary and quaternary structure of surfactant protein A from canine lung, *Biochim. Biophys. Acta 1001*, 294−301.

28. Haagsman, H. P., White, R. T., Schilling, J., Lau, K., Benson, B. J., Golden, J., Hawgood, S., and Clements, J. A. (1989) Studies of the structure of lung surfactant protein SP-A, *Am. J. Physiol. 257*, L421−L429.

29. Putman, E., Creuwels, L. A. J. M., van Golde, L. M. G., and Haagsman, H. P. (1996) Surface properties, morphology and protein composition of pulmonary surfactant subtypes, *Biochem. J. 320*, 599−605.

30. McCormack, F. X., Calvert, H. M., Watson, P. A., Smith, D. L., Mason, R. J., and Voelker, D. R. (1994) The structure and function of surfactant protein A. Hydroxyproline- and carbohydrate-deficient mutant proteins, *J. Biol. Chem. 269*, 5833−5841.

31. Lamberg, A., Helaakoski, T., Myllyharju, J., Peltonen, S., Notbohm, H., Pihlajaniemi, T., and Kivirikko, K. I. (1996) Characterization of human type III collagen expressed in a baculovirus system. Production of a protein with a stable triple helix requires coexpression with the two types of recombinant prolyl 4-hydroxylase subunit, *J. Biol. Chem. 271*, 11988−11995.

32. Mazzorana, M., Snellman, A., Kivirikko, K. I., van der Rest, M., and Pihlajaniemi, T. (1996) Involvement of prolyl 4-hydroxylase in the assembly of trimeric minicollagen XII. Study in a baculovirus expression system, *J. Biol. Chem. 271*, 29003−29008.

33. Brodsky-Doyle, B., Leonard, K. R., and Reid, K. B. M. (1976) Circular-dichroism and electron-microscopy studies of human subcomponent C1q before and after limited proteolysis by pepsin, *Biochem. J. 159*, 279−286.

34. Elhalwagi, B. M., Damodarasami, M., and McCormack, F. X. (1997) Alternate amino terminal processing Surfactant Protein A results in cysteinyl isoforms required for multimer formation, *Biochemistry 36*, 7018−7025.

35. Zhang, M., Damodarasamy, M., Elhalwagi, B. M., and McCormack, F. X. (1998) The longer isoform and Cys^{-1} disulfide bridge of rat Surfactant Protein A are not essential for phospholipid and Type II cell interactions, *Biochemistry 37*, 16481−16488.

36. Schürch, S., Possmayer, F., Cheng, S., and Cockshutt, A. M. (1992) Pulmonary SP-A enhances adsorption and appears to induce surface sorting of lipid extract surfactant, *Am. J. Physiol. 263*, L210−L218.

37. Van Iwaarden, J. F., Pikaar, J. C., Storm, J., Brouwer, E., Verhoef, J., Oosting, R. S., van Golde, L. M. and van Strijp, J. A. (1994) Binding of surfactant protein A to the lipid A moiety of bacterial lipopolysaccharides, *Biochem. J. 303*, 407−411.

38. Benne, C. A., Kraaijeveld, C. A., van Strijp, J. A., Brouwer, E., Harmsen, M., Verhoef, J., van Golde L. M., and van Iwaarden, J. F. (1995) Interactions of surfactant protein A with influenza A viruses: binding and neutralization, *J. Infect. Dis. 171*, 335−341.

39. Benne, C. A., Benaissa-Trouw, B., van Strijp, J. A., Kraaijeveld, C. A., and van Iwaarden, J. F. (1997) Surfactant protein A, but not surfactant protein D, is an opsonin for influenza A virus phagocytosis by rat alveolar macrophages, *Eur. J. Immunol. 27*, 886−890.

40. Van Iwaarden, J. F., van Strijp, J. A., Visser, H., Haagsman, H. P., Verhoef, J., and van Golde, L. M. (1992) Binding of surfactant protein A (SP-A) to herpes simplex virus type 1-infected cells is mediated by the carbohydrate moiety of SP-A, *J. Biol. Chem. 267*, 25039−25043.